A Conservative Discontinuous Galerkin Scheme with $O(N^2)$ Operations in Computing Boltzmann Collision Weight Matrix

Irene M. Gamba[*,†] and Chenglong Zhang[*]

[*] *ICES, The University of Texas at Austin, 201 E. 24th St., Stop C0200, Austin, Texas 78712, USA*
[†] *Department of Mathematics, The University of Texas at Austin, 2515 Speedway, Stop C1200, Austin, Texas 78712, USA*

Abstract. In the present work, we propose a deterministic numerical solver for the homogeneous Boltzmann equation based on Discontinuous Galerkin (DG) methods. The weak form of the collision operator is approximated by a quadratic form in linear algebra setting. We employ the property of "shifting symmetry" in the weight matrix to reduce the computing complexity from theoretical $O(N^3)$ down to $O(N^2)$, with N the total number of freedom for d-dimensional velocity space. In addition, the sparsity is also explored to further reduce the storage complexity. To apply lower order polynomials and resolve loss of conserved quantities, we invoke the *conservation routine* at every time step to enforce the conservation of desired moments (mass, momentum and/or energy), with only linear complexity. Due to the locality of the DG schemes, the whole computing process is well parallelized using hybrid OpenMP and MPI. The current work only considers integrable angular cross-sections under elastic and/or inelastic interaction laws. Numerical results on 2-D and 3-D problems are shown.

Keywords: Boltzmann equation, Discontinuous Galerkin method, Conservative method, Parallel computing
PACS: 51.10.+y, 02.70.Dh, 47.11.Fg

INTRODUCTION

The Boltzmann transport equation (BTE) is of primary importance in rarefied gas dynamics. The numerical approximation to solutions has been a very challenging problem. The main challenges include, but not limited to, the high dimensionality, conservations and complicated collision mechanism.

In history, one category of computational schemes is the well-known *Direct Simulation Monte Carlo* (DSMC) method [1, 2, 3]. DSMC developed to calculate statistical moments under near stationary regimes, but are not efficient to capture details of the solution and will inherit statistical fluctuations. Parallel to the development of DSMC, deterministic methods, such as discrete velocity [4, 5, 6, 7, 8] or spectral methods [9, 10, 11, 12, 13, 14, 15, 16], have been also attracting attentions. For other deterministic schemes, we suggest refer to [17].

The DG [18] method is capable of capturing more irregular features and thus promising to be more powerful in many cases. For problems of charge transport in semiconductor devices, DG methods are very promising and have provided accurate results at a comparable computational cost [19, 20]. It seems, DG could be a potential method for kinetic equations. However, there are very rare work on full nonlinear Boltzmann model [21, 22]. Our scheme was developed independently and is different than any work mentioned ahead, in the way of constructing basis functions, evaluating angular cross-section integrals and the enforcing of conservation routines.

The remaining paper is organized as follows. The homogeneous Boltzmann equation is introduced. After that, we introduce the numerical projection of the collision operator onto the DG mesh. Then, techniques on reducing the complexity are explained. Before showing numerical results, the conservation routine is described. The summary and future work are outlined in the last section.

THE SPACE HOMOGENEOUS BOLTZMANN EQUATION

The Boltzmann equation is an integro-differential equation, with the solution a phase probability density distribution. Since most technical challenges come from the treatment of the collision operator, our current work only focuses on the homogeneous equation, which is given by

$$\frac{\partial f(v,t)}{\partial t} = Q(f,f)(v,t) \tag{1}$$

with initial $f(v,0) = f_0(v$. Here the bilinear integral collision operator, can be defined weakly or strongly. The strong form goes

$$Q(f,f) = \int_{v_*\in\mathbb{R}^d,\sigma\in\mathbb{S}^{d-1}} [f'f'_* - ff_*]\, B(|v-v_*|,\sigma)\, d\sigma dv_*\,, \tag{2}$$

where $f = f(v)$, $f_* = f(v_*)$ and $f' = f(v')$, $f'_* = f(v'_*)$, v', v'_* are pre-collisional velocities, following the elastic collision law (though this solver can be easily extended to inelastic cases)

$$u = v - v_*, \quad v' = v + \frac{1}{2}(|u|\sigma - u), \quad v'_* = v_* - \frac{1}{2}(|u|\sigma - u)\,. \tag{3}$$

The *collision kernel*

$$B(|u|,\sigma) = |u|^\gamma b(\cos(\theta)), \quad \gamma \in (-d, +\infty)\,, \tag{4}$$

models the intermolecular potentials and the *angular cross-sections*

$$\cos(\theta) = \frac{u\cdot\sigma}{|u|}\,, \quad b(\cos(\theta)) \sim \sin^{-(d-1)-\alpha}(\frac{\theta}{2}) \text{ as } \theta \sim 0\,, \quad \alpha \in (-\infty, 2) \tag{5}$$

The weak form for (2), or called Maxwell form, after a change of variable $u = v - v_*$ is given by

$$\int_{\mathbb{R}^d} Q(f,f)(v)\phi(v)dv = \int_{v,u\in\mathbb{R}^d} f(v)f(v-u)\int_{\sigma\in S^{d-1}} [\phi(v') - \phi(v)]B(|u|,\sigma)d\sigma du dv\,, \tag{6}$$

which is a *double mixing convolution*. Also see spectral methods [14, 15] .

THE DISCONTINUOUS GALERKIN PROJECTIONS

We are working in the velocity domain $v \in \Omega_v = [-L, L]^d$. A regular mesh is applied, that is, we divide each direction into n disjoint elements uniformly, such that $[-L, L] = \bigcup_k I_k$, where interval $I_k = [w_{k-\frac{1}{2}}, w_{k+\frac{1}{2}})$, $w_k = -L + (k+\frac{1}{2})\Delta v$, $\Delta v = \frac{2L}{n}$, $k = 0 \ldots n-1$ and thus there is a Cartesian partitioning $\mathcal{T}_h = \bigcup_k E_k$, with uniform cubic element $E_k = I_{k_1} \otimes I_{k_2} \ldots \otimes I_{k_d}$, $k = (k_1, k_2, ..., k_d)$.

Discontinuous Galerkin methods assume piecewisely defined basis functions, that is

$$f(v,t) = \sum_k \mathbf{u}_k(t)\cdot\Phi(v)\chi_k(v), \tag{7}$$

where multi-index $k = (k_1, k_2, ..., k_d)$, $0 \le |k| < (n-1)^3$; $\chi_k(v)$ is the characteristic function over element E_k; coefficient vector $\mathbf{u}_k = (\mathbf{u}_k^0, ..., \mathbf{u}_k^p)$, where p is the total number of basis functions locally defined on E_k; basis vector $\Phi(v) = (\phi_0(v), ..., \phi_p(v))$. Usually, we choose element of basis vector $\Phi(v)$ as local polynomial in $P^p(E_k)$, which is the set of polynomials of total degree at most p on E_k. For sake of convenience, we select the basis such that $\{\phi_i(v) : i = 0, ..., p\}$ are orthogonal.

Apply the i-th basis function on element E_m, $\phi_i(v)\chi_k(v)$, to (6) and operate a change of variables $(v,u) \leftarrow (v, v_*)$, where $u = v - v_*$ is the relative velocity,

$$\begin{aligned}
&\int_{v\in E_m} Q(f,f)\phi_i(v)dv \\
&= \int_{v\in E_m, v_*\in\mathbb{R}^d} f(v)f(v-u)\int_{\sigma\in\mathbb{S}^{d-1}} [\phi_i(v')\chi_m(v') - \phi_i(v)\chi_m(v)]|u|^\gamma b(\frac{u\cdot\sigma}{|u|})d\sigma du dv \\
&= \sum_k \sum_{\bar{k}} \mathbf{u}_k^T \mathbf{G}_{m,i}(k,\bar{k})\mathbf{u}_{\bar{k}}\,.
\end{aligned} \tag{8}$$

Here, for fixed $k,\bar{k},m,i$, the entry $\mathbf{G}_{m,i}(k,\bar{k})$ is actually a $(p+1)\times(p+1)$ matrix, defined as

$$\begin{aligned}&\mathbf{G}_{m,i}(k,\bar{k})=\\&\int_{v\in E_k}\int_{v-u\in E_{\bar{k}}}\Phi(v)\otimes\Phi(v-u)\chi_k(v)\chi_{\bar{k}}(v-u)|u|^\gamma\int_{\mathbb{S}^{d-1}}[\phi_i(v')\chi_m(v')-\phi_i(v)\chi_m(v)]b(\tfrac{u\cdot\sigma}{|u|})d\sigma du dv\,.\end{aligned}\tag{9}$$

The key is to evaluate the block entry $\mathbf{G}_{m,i}(k,\bar{k})$ in (9). Due to the convolution formulation, the integrals w.r.t v,u can be approximated through *Triangular quadratures*. The integrals on the sphere take the most effort. To save the tremendous computational work on evaluating the angular integrals, one has to figure out the "effective integration domains" where the integrand of angular integrals in (9) is continuous. Finally, over each "effective" domain, the angular integrations are performed by adaptive quadratures.

REDUCTIONS ON THE COMPUTING AND STORAGE COMPLEXITY OF COLLISION MATRIX

Theoretically, the computing and storage complexity for the weight matrices $\mathbf{G}_{m,i}$ would be $O(N^3)$, with $N=(p+1)n$. However, the following features are applied to reduce the cost, i.e temporally independent and precomputed, shifting symmetric, sparse and parallelizable.

Shifting Symmetry Property for Uniform Meshes

Here we assume a uniform mesh. Recall the post-collisional velocity $v'=\frac{v+v_*}{2}+\frac{|v-v_*|}{2}\sigma$. Thus, as long as the relative positions between E_k ($E_{\bar{k}}$) and test element E_m keep unchanged, and at the same time, the piecewise basis functions $\phi(v)$ on E_m are only valued locally upon the relative position of v inside E_m, then (9) will be unchanged. This is summarized as the following theorem.

Theorem (Shifting Symmetry)**.** *If the basis piecewise polynomials $\phi(v)$, defined over element E_m, are functions of $\frac{v-w_m}{\Delta v}$ (where w_m is the center of cube E_m), then, the family of collision matrix $\{\mathbf{G}_{m,i}\}$ satisfies the "shifting symmetry" property*

$$\mathbf{G}_{m,i}(k,\bar{k})=\mathbf{G}_{\tilde{m},i}(k-(m-\tilde{m}),\bar{k}-(m-\tilde{m})),\tag{10}$$

where $m,\tilde{m},k,\bar{k}$ are d-dimensional multi-indices; $i=0,\ldots,p$.

This shifting procedure can be illustratively shown in Figure 1. Figure 1 shows that the lower-right $(n-1)\times(n-1)$ submatrix of Matrix G_1 is equivalent to the upper-left submatrix of Maxtrix G_0, while only leaving the first row and column of G_1 to be determined. This rule applies again to Matrix G_2.

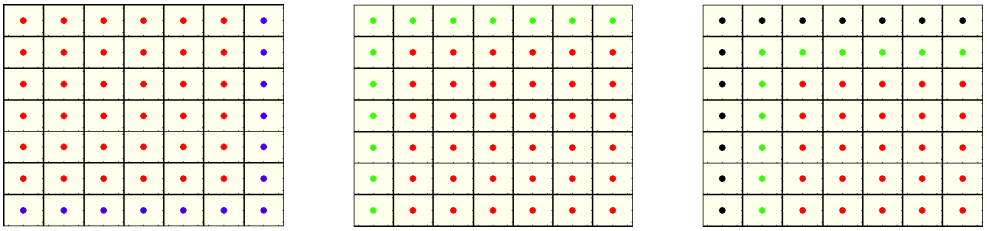

Matrix G_0 Matrix G_1 Matrix G_2

FIGURE 1. Dots (entries) of the same color are shifted to the neighboring matrices, showing illustratively for 1-D

This implies the existence of a basis set of matrices, which can be defined in the following theorem.

Theorem (Minimal Basis Set)**.** *There exists a minimal basis set of matrices*

$$\mathfrak{B}=\{G_{m,i}(k,\bar{k}):\textit{For } j=1..d,\ \textit{if } m_j\neq 0,k_j\times\bar{k}_j=0;\ \textit{if } m_j=0,k_j,\bar{k}_j=0,1,\ldots,n-1\},$$

which can exactly reconstruct the complete family $\{\mathbf{G}_{m,i}\}$, through shifting.

Therefore, along each dimension, we only need to compute and store the full matrix for $m=0$, and the first rows and columns for all other m's. This requires a computing complexity of only $O(N^2)$.

Sparsity

The sparsity of $\mathfrak{B}$, again, comes from $v' = v - \frac{u}{2} + \frac{|u|}{2}\sigma$. The post-collisional velocity v' is on the sphere with center and radius given by v, u. Thus, not all binary particles, with velocity $v \in E_k$ and $v_* \in E_{\bar{k}}$, could collide ending up with a post-collisional velocity v' lying in a given element E_m. It counts only when the sphere intersects with element E_m, resulting in only $O(n^{2d-1})$ nonzeros in the set $\mathfrak{B}$.

Therefore, in practice, we obtain computing complexity $O(n^{2d})$ and storage complexity $O(n^{2d-1})$. The table 1 are test runs for $d = 3$ on a single core of Xeon E5-2680 2.7GHz processor (on cluster Stampede-TACC [23]), which verify our observations.

TABLE 1. The computing and storage complexity of "basis" $\mathfrak{B}$.

n	wall clock time (s)	order	number of nonzeros	order
8	3.14899	\	812884	\
12	39.3773	6.2301	6826904	5.2484
16	228.197	6.1075	30225476	5.1717
20	893.646	6.1176	94978535	5.1311
24	2686.72	6.0375	241054134	5.1054

Parallelization

Due to the locality of DG basis functions, the whole process of computing $\mathfrak{B}$ can be well performed using hybrid MPI [24] and OpenMP [25]. Figure 2 shows the parallel efficiency of strong scaling for computing some sets of "basis matrix".

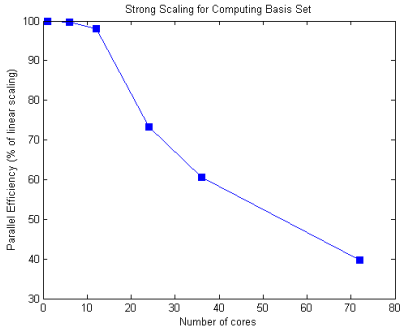

FIGURE 2. The strong scalability of computing collision matrix (n=18)

CONSERVATION ROUTINES

The above approximate collision operator Q doesn't preserve the moments as needed, mainly due to the DG approximation and domain truncation. Following the ideas in [14], we introduce a *L^2-distance minimization problem* with the constraints the preservation of desired moments, as follows,

Conservation Routine [Discrete Level]: Find $\mathbf{Q}_c$, the minimizer of the problem

$$\begin{aligned} &\min \frac{1}{2}(\mathbf{Q}_c - \mathbf{Q})^T \mathbf{D}(\mathbf{Q}_c - \mathbf{Q}) \\ &\text{s.t.} \quad \mathbf{C}\mathbf{Q}_c = \mathbf{0}. \end{aligned}$$

where the $(d+2) \times N$ dimensional constraint matrix writes

$$\mathbf{C}_{:,j} = \begin{pmatrix} \int_{E_k} \phi_l(v) dv \\ \int_{E_k} \phi_l(v) v dv \\ \int_{E_k} \phi_l(v) |v|^2 dv \end{pmatrix}, \tag{11}$$

with ϕ_l the $l-th$ basis function on element E_k and the column index $j=(p+1)k+l=0,\ldots,N-1$. Due to the orthogonality of the local basis, $\mathbf{D}$ is a positive definite diagonal matrix with its j-th entry $\frac{1}{|E_k|}\int_{E_k}(\phi_l(v))^2dv$, $j=(p+1)k+l$.

We employ the Lagrange multiplier method and obtain the minimizer $\mathbf{Q}_c$

$$\mathbf{Q}_c=[\mathbf{I}-\mathbf{D}^{-1}\mathbf{C}^T(\mathbf{C}\mathbf{D}^{-1}\mathbf{C}^T)^{-1}\mathbf{C}]\mathbf{Q}, \tag{12}$$

where $\mathbf{I}$ is an identity matrix of size $N\times N$. Hence, $\mathbf{Q}_c$ is a perturbation of $\mathbf{Q}$.

Therefore, the final conservative semi-discrete DG formulation for the homogeneous equation writes

$$\frac{d\mathbf{U}}{dt}=\mathbf{Q}_c\,. \tag{13}$$

The solution (13) approaches a stationary state, guaranteed by analyzing the convergence behavior.

TEMPORAL EVOLUTION

Since there is no CFL condition imposed, the first order *Euler scheme* is sufficient. At each time step, the conservation routine, denoted by *CONSERVE*, will be called. Suppose $\mathbf{U}_n$ is the coefficient vector (thus the solution) computed at the current time t_n, then the solution for the next time step is obtained through the following routines

$$\begin{aligned}&\mathbf{Q}_n=\text{COMPUTE}(\mathbf{U}_n)\,,\\&\mathbf{Q}_{c,n}=\text{CONSERVE}(\mathbf{Q}_n)\,,\\&\mathbf{U}_{n+1}=\mathbf{U}_n+\triangle t\mathbf{Q}_{c,n}\,.\end{aligned}$$

For higher order accuracy, a higher order Runge Kutta scheme can be used whenever necessary. The conservation routine has to be invoked at every intermediate step of the Runge Kutta scheme.

At each time step, the actual order of number of operations for each time step is $O(n^8)$. Fortunately, the reconstructions of collision matrices and computing of quadratic form (8) are well parallelizable for each Euler step.

NUMERICAL RESULTS

Test 1 is a 2-d Maxwell model ($\alpha=-1$, $\gamma=0$) with elastic collisions, benchmarked by *Bobylev-Krook-Wu (BKW)* exact solutions. The initial density distribution is

$$f(v,0)=\frac{v^2}{\pi\sigma^2}\exp(-v^2/\sigma^2)\,, \tag{14}$$

with $\sigma=\pi/6$. This problem has an exact solution [26]

$$f(v,t)=\frac{1}{2\pi s^2}\left(2s-1+\frac{1-s}{2s}\frac{v^2}{\sigma^2}\right)\exp\left(-\frac{v^2}{2s\sigma^2}\right), \tag{15}$$

We select truncated domain $\Omega_v=[-\pi,\pi]$. Figure 3 shows the DG solutions agree very well with the exact ones and the convergence of relative entropy. The relative entropy is given by

$$\mathcal{H}_{rel}(t)=\int_{\Omega_v}f(v,t)\log f(v,t)-f_M(v)\log f_M(v)dv=\int_{\Omega_v}f(v,t)\log\frac{f(v,t)}{f_M(v)}dv\,, \tag{16}$$

where $f_M(v)$ is the true equilibria. The convergence to zero implies the solution converges to the true equilibria in the sense of L^1.

Test 2 is also 2-d Maxwell model with elastic collisions. This example is to justify the conservation routines. The initial density function is a convex combination of two Maxwellians

$$f_0(v)=\lambda M_1(v)+(1-\lambda)M_2(v)\,, \tag{17}$$

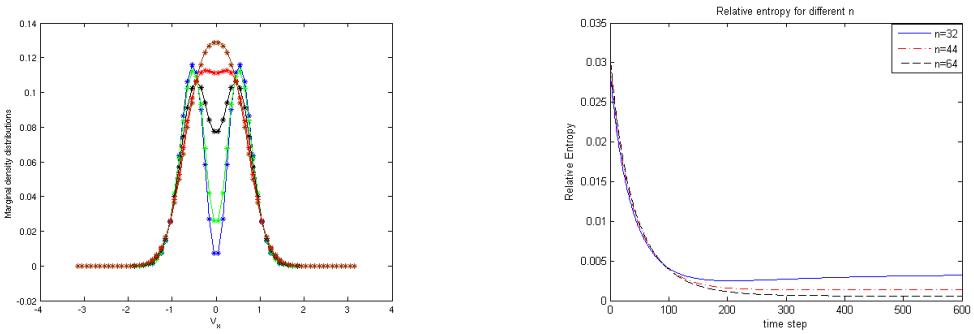

FIGURE 3. **Test 1**: Left: solutions at time $t = 0, 1, 5, 10, 15s$. n=44. solid line: exact solution, stars: DG solution; Right: relative entropy for different n

with $M_i(v) = (2\pi T_i)^{-d/2} e^{-\frac{|v-V_i|^2}{2T_i}}$, $T_1 = T_2 = 0.16$, $V_1 = [-1, 0]$, $V_2 = [1, 0]$ and $\lambda = 0.5$.

Truncate the velocity domain $\Omega = [-4.5, 4.5]^2$. We test for $n = 32$ and $n = 40$ with piecewise constant test functions. The probability density distribution functions are reconstructed with splines.

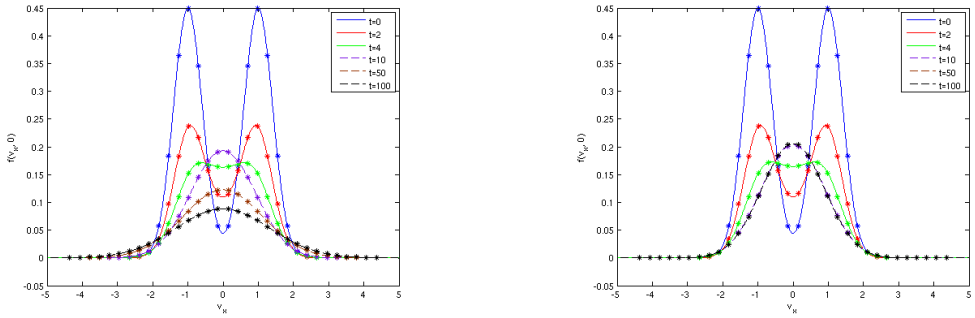

FIGURE 4. **Test 2**: Evolution of pdf without (left) and with (right) conservation routines

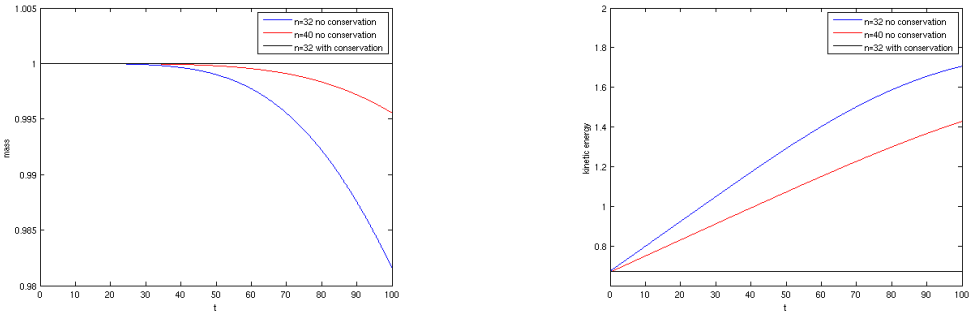

FIGURE 5. **Test 2**: Evolution of mass (left) and kinetic energy (right)

Figure 4 shows, after long time, with no conservation routine, the density distribution collapses. While with conservation routines, the density function stays stable after equilibrium. Figure 5 shows the evolution of moments up to the second order with and without conservation routines.

Test 3 is initialized by a sudden jump on temperatures, given by

$$f_0(v) = \begin{cases} \dfrac{1}{2\pi T_1} \exp(-\dfrac{|v|^2}{2T_1}), & v_1 \le 0 \\ \dfrac{1}{2\pi T_2} \exp(-\dfrac{|v|^2}{2T_2}), & v_1 > 0 \end{cases}$$

in case of $d=2$, $\alpha=-1$, $\gamma=1$. Here, We select $T_1=0.3$ and $T_2=0.6$, domain $\Omega_v=[-5,5]$, $n=44$ in each direction. Figure 6 indicates that the DG solution well captures the discontinuity and converges to equilibrium.

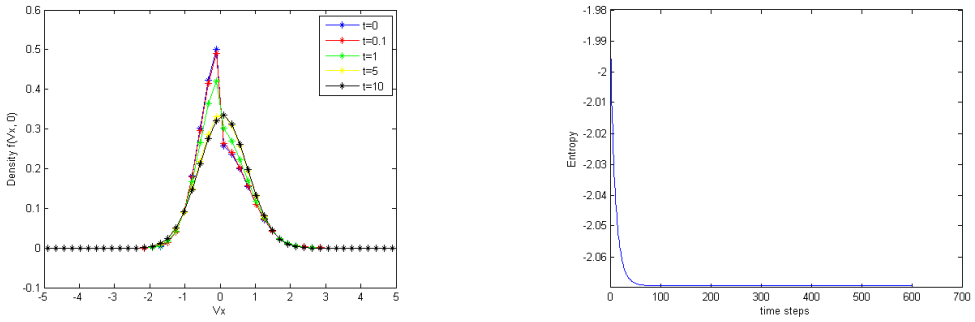

FIGURE 6. **Test 3**: The DG solutions (left) and entropy decay (right)

Test 4 is testing on the 3D homogeneous Boltzmann equation with Maxwell molecular potential ($\alpha=-2$, $\gamma=0$), with initial

$$f_0(v)=\frac{1}{2(2\pi\sigma^2)^{3/2}}\left[\exp\left(-\frac{|v-2\sigma e|^2}{2\sigma^2}\right)+\exp\left(-\frac{|v+2\sigma e|^2}{2\sigma^2}\right)\right],$$

where parameters $\sigma=\pi/10$ and $e=(1,0,0)$. We select $\Omega_v=[-3.4,3.4]^3$, $n=30$.

Figure 7 shows the evolution of the marginal density distributions. Figure 8 shows the entroy decay and

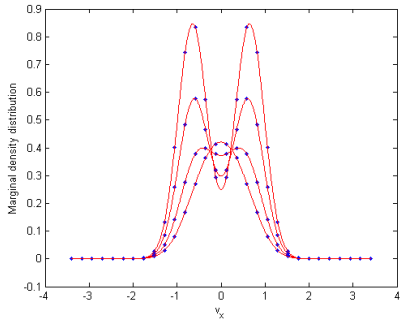

FIGURE 7. **Test 4**: Evolution of marginal distributions at $t=0,1,2.5,5s$; dots are the piecewise constant value on each element; solid lines are spline reconstructions

relaxations of directional temperature, which as expected converge to the averaged temperature.

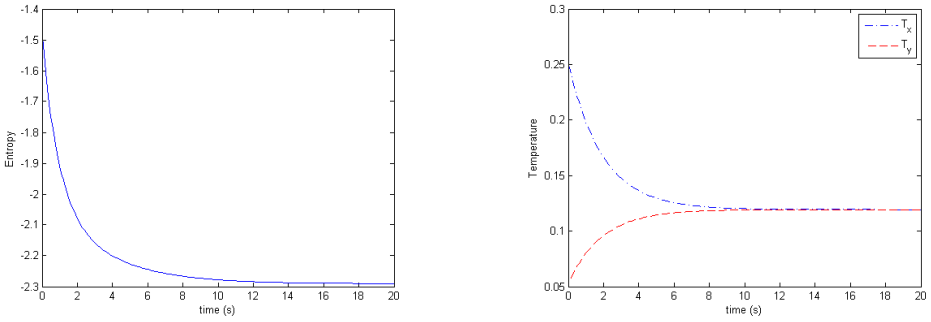

FIGURE 8. **Test 4**: Entropy decay (left) and temperature relaxations along x and y directions (right)

SUMMARY AND FUTURE WORK

We proposed a deterministic numerical solver for the homogeneous Boltzmann equation, based on DG method. The shifting symmetry property and sparsity are employed to reduce the computing complexity for the collision weight matrix down to $O(n^{2d})$ from $O(n^{3d})$ and the storage complexity down to $O(n^{2d-1})$. The conservation routine is also designed to enforce the inclusion of the collision invariants in the null space of the approximated collision operator. Thanks to the locality of DG meshes, the whole computing process is parallelized with hybrid OpenMP and MPI. In future, we hope to speedup the numerical temporal evolution, to increase the accuracy of approximating collision integrals and also to incorporate with the advection term to study space inhomogeneous Boltzmann problems.

ACKNOWLEDGMENTS

This work has been supported by ...

REFERENCES

1. G. Bird, *Molecular Gas Dynamics*, Clarendon Press, Oxford, 1994.
2. K. Nanbu, *J. Phys. Soc. Japan* **52**, 2042–2049 (1983).
3. S. Rjasanow, and W. Wagner, *Stochastic Numerics for the Boltzmann Equation*, Springer, Berlin, 2005.
4. J. E. Broadwell, *J. Fluid Mech.* **19**, 401–414 (1964).
5. H. Cabannes, *Comm. Math. Phys* **74**, 71–95 (1980).
6. R. Illner, *J. de Mecanique* **17**, 781–796 (1978).
7. S. Kawashima, *Proc. Japan Acad. Ser. A Math. Sci.* **57**, 19–24 (1981).
8. A. Morris, P. Varghese, and D. Goldstein, "Variance Reduction for a Discrete Velocity Gas," in *27th International Symposium on Rarefied Gas Dynamics 2010*, AIP Conf. Proc. 1333, 2011.
9. A. V. Bobylev, and S. Rjasanow, *European journal of mechanics. B, Fluids* **16**, 293–306 (1997).
10. A. V. Bobylev, and C. Cercignani, *Journal of Statistical Physics.* **97**, 677–686 (1999).
11. L. Pareschi, and G. Russo, *SIAM J. Numerical Anal. (Online)* **37**, 1217–1245 (2000).
12. A. V. Bobylev, *Translated from Teoreticheskaya i Mathematicheskaya Fizika* **60**, 280–310 (1984).
13. F. Filbet, C. Mouhot, and L. Pareschi, *SIAM J. Sci. Comput.* **28**, 1029–1053 (2006).
14. I. Gamba, and S. H. Tharkabhushaman, *Journal of Computational Physics* **228**, 2012–2036 (2009).
15. I. Gamba, and S. H. Tharkabhushaman, *Jour. Comp. Math* **28**, 430–460 (2010).
16. J.R.Haack, and I. Gamba, *28th Rarefied Gas Dynamics Conference (2012)* (AIP Conference Proceedings (2012)).
17. V. V. Aristov, *Direct methods for solving the Boltzmann equation and study of nonequilibrium flows*, Kluwer Academic Publishers, Dordrecht, 2001.
18. B. Cockburn, and C.-W. Shu, *Journal of Scientific Computing* **16**, 173–261 (2001).
19. Y. Cheng, I. Gamba, A. Majorana, and C.-W. Shu, *Comput. Methods Appl. Mech. Engrg* **198**, 3130–3150 (2009).
20. Y. Cheng, I. Gamba, A. Majorana, and C.-W. Shu, *AIP Conference Proceedings* **1333**, 892–895 (2011).
21. A. Majorana, *Kinetic and Related Models* **4**, 139–151 (2011).
22. A. Alekseenko, and E. Josyula, *Journal of Computational Physics* (submitted).
23. T. U. of Texas at Austin, Texas advanced computing center (TACC), `http://www.tacc.utexas.edu`.
24. E. Gabriel, G. Fagg, G. Bosilca, T. Angskun, J. J. Dongarra, J. M. Squyres, V. Sahay, P. Kambadur, B. Barrett, A. Lumsdaine, R. H. Castain, D. J. Daniel, R. L. Graham, and T. S. Woodall, "Open MPI: Goals, Concept, and Design of a Next Generation MPI Implementation," in *Proceedings, 11th European PVM/MPI Users' Group Meeting*, Budapest, Hungary, 2004, pp. 97–104.
25. O. A. R. Board, OpenMP application program interface version 3.0 (2008), `http://www.openmp.org/mp-documents/spec30.pdf`.
26. M. Ernst, *Exact solutions of the nonlinear Boltzmann equation and related kinetic models, Nonequilibrium Phenomena, I, Stud. Statist. Mech. 10*, North-Holland, Amsterdam, 1983.